

Numerical investigation of cavitation processes

Nadezhda L. Zagordan Dmitry L. Reviznikov
zagordann@gmail.com

Abstract

Numerical simulation approach addressing problems of cavitation processes and vapor-liquid two-phase flow dynamics research is discussed. The Navier-Stokes equations, supplemented by transport equation containing source terms, responsible for the interphase exchange, are solved to obtain hydrodynamic characteristics of the system. A comparative analysis of the experimental data and computational results is carried out for different regimes of cavitating flows inside a two-dimensional nozzle with variable cross-section. The oscillation characteristics of hydrodynamic parameters and the gas-vapor bubbles behavior are investigated.

1 Introduction

Nowadays technologies utilizing the hydrodynamic and thermophysical effects of cavitation have received wide spread in various branches of industry. Recent improvements in measuring techniques have led to a numerous experimental studies of two-phase flows. However, the detailed data on the properties of the flows, containing bubbles as a dispersed phase, are difficult to obtain experimentally. Therefore, numerical simulations are extensively used for collecting accurate information on two-phase mixture parameters. At present, a number of mathematical models have been proposed to describe vapor-liquid flows. Most of them treat the two-phase flow as a homogeneous vapor-liquid mixture. Though there are studies dedicated to cryogenic cavitation simulation, the majority of models make an assumption of isothermal conditions. Barotropic equations of state have been proposed to link the density of vapor-liquid mixture and the local pressure. However, as noted by Senocak and Shyy [1], use of barotropic relation makes the baroclinic torque vanish and this result contradicts experimentally measured data on thermal physical vorticity in cavitating flows [2]. Another common approach to generate variable density field is to solve transport equation for volume fraction with condensation and evaporation source terms controlling the mass transfer between two phases.

The present study is aimed at numerical investigating of two-phase viscous flow characteristics. Comparative analysis of the experimental data and computational results is used as a validation benchmark for cavitating flow modeling.

2 Mathematical model

A planner two-phase viscous flow is governed by time-dependent Navier-Stokes equations and a transport equation, solved to account for a phase exchange:

$$\left\{ \begin{array}{l} \frac{\partial(\rho_m u)}{\partial t} + \frac{\partial}{\partial x}(\rho_m u^2 - \mu \frac{\partial u}{\partial x}) + \frac{\partial}{\partial y}(\rho_m uv - \mu \frac{\partial u}{\partial y}) = -\frac{\partial p}{\partial x} \\ \frac{\partial(\rho_m v)}{\partial t} + \frac{\partial}{\partial x}(\rho_m uv - \mu \frac{\partial v}{\partial x}) + \frac{\partial}{\partial y}(\rho_m v^2 - \mu \frac{\partial v}{\partial y}) = -\frac{\partial p}{\partial y} \\ \frac{\partial \rho_m}{\partial t} + \frac{\partial(\rho_m u)}{\partial x} + \frac{\partial(\rho_m v)}{\partial y} = 0 \\ \frac{\partial \alpha}{\partial t} + \frac{\partial(\alpha u)}{\partial x} + \frac{\partial(\alpha v)}{\partial y} = \dot{m}^+ + \dot{m}^- \\ \rho_m = \alpha \rho_L + (1 - \alpha) \rho_v \end{array} \right. \quad \begin{array}{l} (1) \\ (2) \\ (3) \\ (4) \\ (5) \end{array}$$

where t is the time, u and v are components of velocity, p is the pressure, ρ_m is the mixture density, ρ_v is the vapor density, α is the liquid volume fraction, \dot{m}^- is the source term for evaporation, \dot{m}^+ is the source term for condensation. Source terms \dot{m}^- and \dot{m}^+ are the functions of pressure and contain empirical coefficients C_{dest} and C_{prod} regulating the rate of condensation and evaporation [3]:

$$\dot{m}^+ = \frac{C_{prod} \max(p - p_{cav}, 0)(1 - \alpha)}{(0.5 \rho_L U_\infty^2) t_\infty}, \quad \dot{m}^- = -\frac{C_{dest} \rho_L \min(p - p_{cav}, 0) \alpha}{\rho_L (0.5 \rho_L U_\infty^2) t_\infty} \quad (6)$$

where U_∞ is the free stream velocity, $t_\infty = \frac{L_N}{U_\infty}$ is the characteristic time scale; L_N is the characteristic length of the nozzle; p_{cav} is the vapor saturation pressure.

Modified PISO algorithm ([4], [5]) has been utilized to couple the continuity and momentum equations. The discretized equations have been obtained using control volume technique on staggered grid mesh. The convergence behavior of some SIMPLE-like algorithms is known to be strongly affected by the choice of the under-relaxation parameters. It should be noted that the present algorithm provides reliable convergence without introduction of the under-relaxation coefficients.

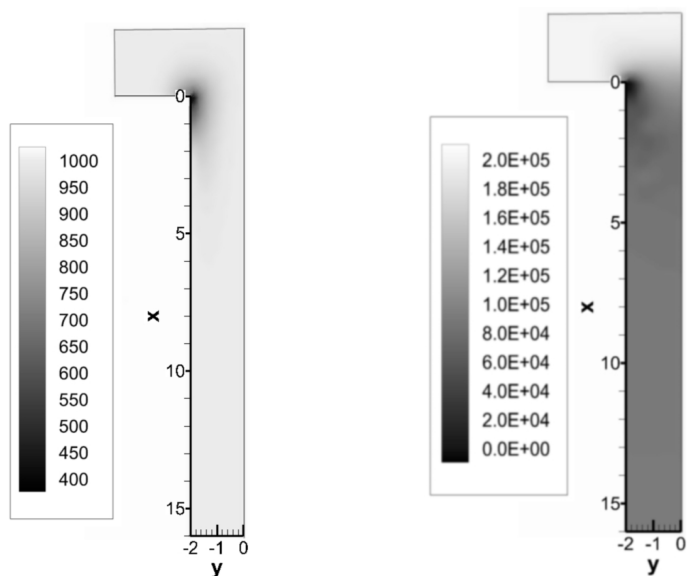
3 Analysis of results

A comparative analysis of the experimental data [6] and computational results has been carried out for different cavitation regimes in order to verify suggested models. Two-phase flow with kinematic viscosity of $10^{-6} \frac{m^2}{s}$ running through a two-dimensional nozzle 23 mm long is simulated. The nozzle used in the experiment is composed of an inlet 32 mm wide and a narrow outlet 4 mm wide and 16 mm long. The computational domain corresponds to a half of the nozzle due to the vertical symmetry of the flow. The cavitation number is defined by the formula: $\sigma = \frac{p_a - p_{cav}}{0.5 \rho_L U_N^2}$ [6], here p_a denotes the atmospheric pressure and U_N is the liquid velocity in the nozzle averaged over the area.

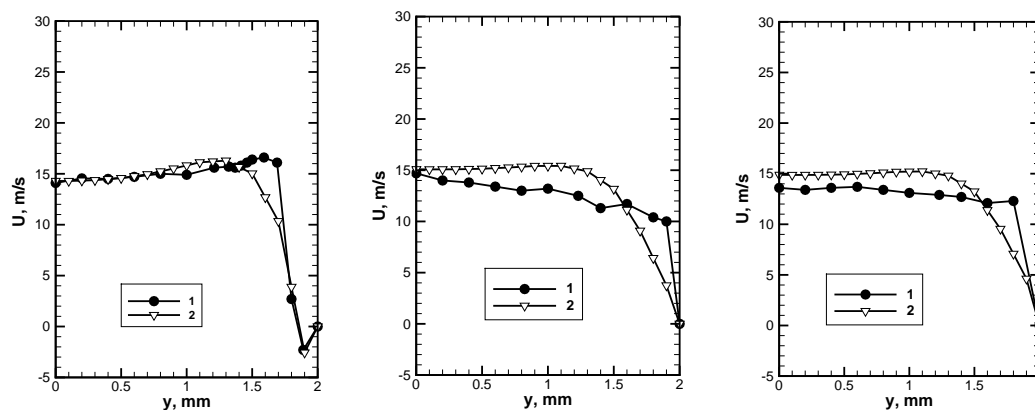
The simulations are performed for the flow at various cavitation regimes [5]. In this paper the computation results for incipient cavitation and super-cavitation regimes are obtained using cavitation numbers of $\sigma = 1.27$ and $\sigma = 0.65$. The laminar model is used to simulate the flow.

Calculated instantaneous flow fields of hydrodynamic characteristics in the incipient cavitation regime ($\sigma = 1.27$) are shown in Figure 1. Inlet pressure drops to the critical value in proximity to the nozzle; this causes the vapor phase to be produced in this region.

Experimentally measured [6] and computed longitudinal velocities are shown in Figure 2. It can be seen that the agreement between the velocity profiles is reasonably good


 (a) Density field, kg/m^3

(b) Pressure field, Pa

 Figure 1: Hydrodynamic parameter distributions at $\sigma = 1.27$

 (a) $x = 0.5$ mm section

 (b) $x = 8$ mm section

 (c) $x = 13$ mm section

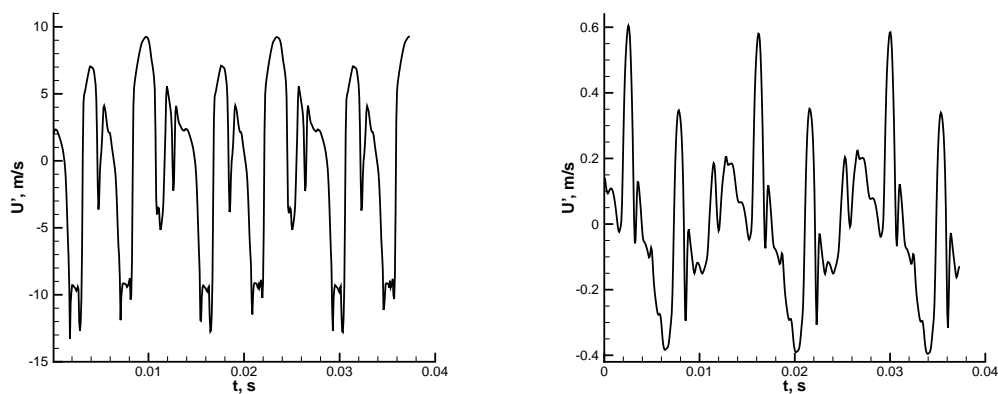
 Figure 2: Time-averaged velocity distributions at $\sigma = 1.27$.

1 – experimentally measured velocities; 2 – calculated velocities

for the first cross section (Figure 2a), where the cavitation regime is observed. Downstream the disagreement, caused by the use of the laminar flow model, may be observed.

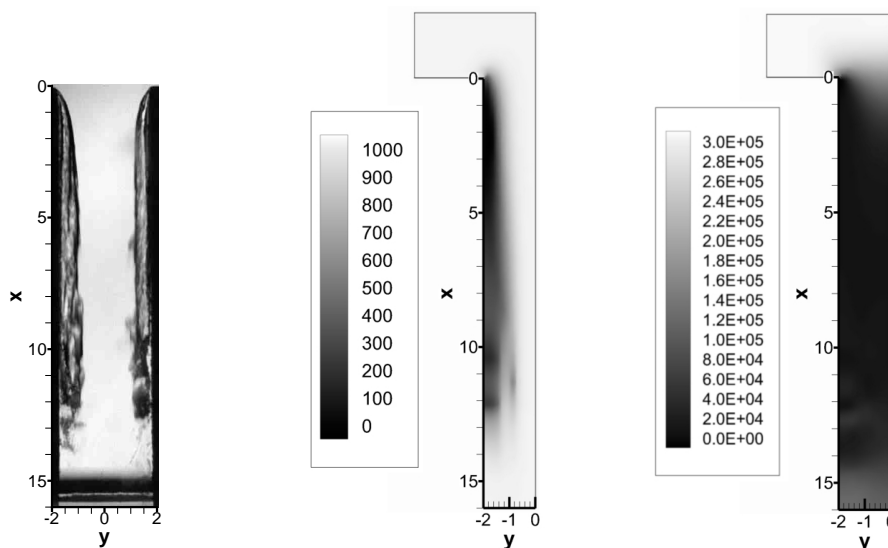
Numerical experiments indicate that the incipient cavitation provokes periodic flow oscillations. Figure 3 illustrates computed absolute longitudinal velocity variance u' of time averaged velocity u in the section $x = 0.5$ mm. The velocity variance is measured at different off-axis points.

Increase of liquid consumption results in the extension of the low pressure area and the growth of vapor phase content. However, the core area of the nozzle is almost homogeneous and contains practically no vapor phase. At the same time the vapor content is high within the boundary layer of the flow. Experimental flow image and computed instantaneous density and pressure fields in the super-cavitation regime with $\sigma = 0.65$ are shown in Figure 4. Figure 5 represents the distributions of experimentally measured and computed velocities. It can be seen that experimental data and computational results are in a close agreement for both cavitation zone size and velocity profiles.



(a) 1.9 mm distant from the longitudinal axis (b) 0.7 mm distant from the longitudinal axis

Figure 3: Absolute longitudinal velocity variance of time averaged velocity in the section $x = 0.5$ mm, $\sigma = 1.27$

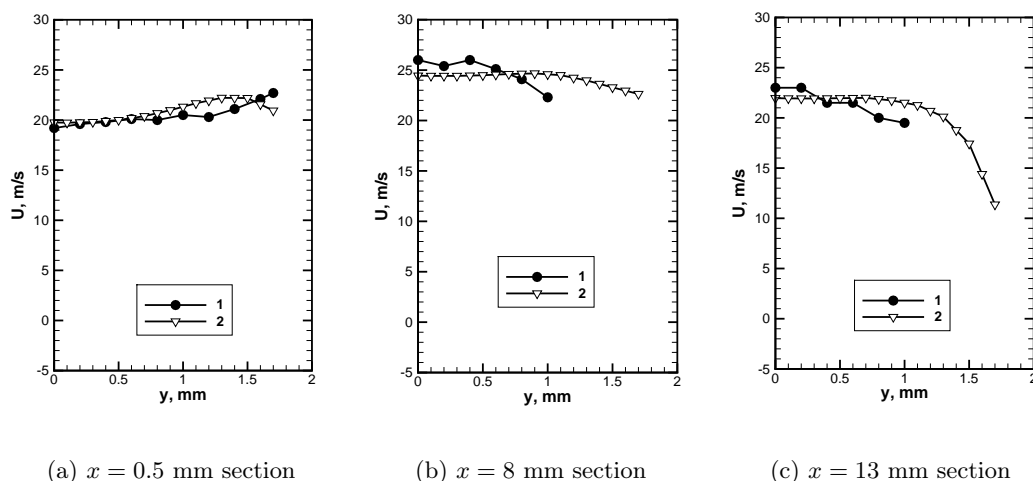


(a) Photograph of a flow (b) Density field, kg/m^3 (c) Pressure field, Pa

Figure 4: Hydrodynamic parameter distributions at $\sigma = 0.65$

Figure 6 illustrates the standard deviation of experimentally measured and calculated velocities u from the time-averaged velocities for regimes with cavitation numbers $\sigma = 1.27$ and $\sigma = 0.65$. In both the incipient cavitation regime and the super-cavitation regime the best agreement of velocity fluctuations with experimental data was obtained along the side walls, whereas fluctuations calculated for the central zone are much weaker than those experimentally measured. Thus, two types of the oscillating motion of vapor-liquid mixture may be distinguished. Pulsations of the cavitation origin dominate in the region with high vapor content and are reliably reproduced in the computational experiments. It can be seen from Figure 6 that cavitation pulsations decay near to the longitudinal axis and turbulent pulsations appear to play the dominant role. It should be pointed out that the oscillations take on the chaotic character in the super-cavitation regime (see Figure 7). It should be noted also that Nazarov [7] experiments detected the change in sound characteristics at the moment of full flow separation.

Figure 8 shows the dimensionless cavitation zone length L_{cav} dependence on the pres-


 Figure 5: Time-averaged velocity distributions at $\sigma = 0.65$.

1 – experimentally measured velocities; 2 – calculated velocities

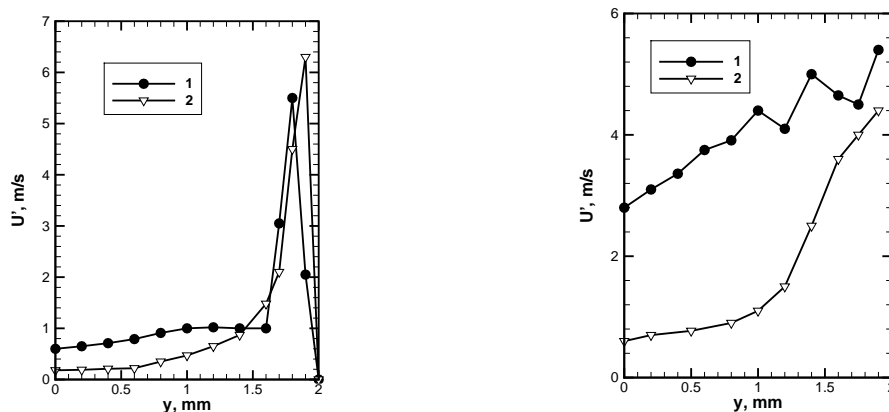


Figure 6: Standard deviation of velocities from the time-averaged values.

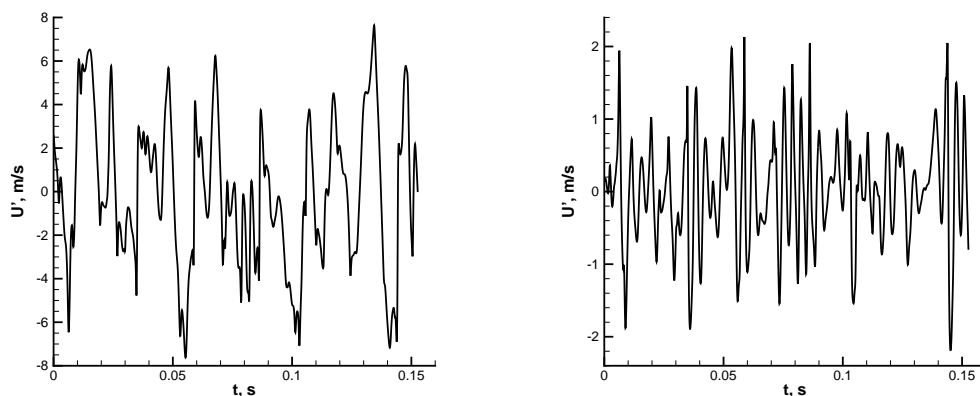
1 – experiment; 2 – simulation

sure differential across the nozzle dP , where L_{cav} is the ratio of the absolute cavitation zone length L_{cav} and the length of the narrow section of the nozzle L_N . It can be seen that the agreement between the experiment and the computations is quite good.

4 Conclusions

In this paper, the comparative analysis of experimental data and computational results was carried out for different cavitation regimes. Close agreement between the experimental data and the computational results for both size of cavitation area and velocity profiles in cavitation zones has been obtained.

Furthermore, the oscillating character of hydrodynamic parameters of cavitating flows was investigated. It was found that the periodic oscillations prevail in the incipient cavitation regime and the chaotic pulsations are typical for super-cavitation regime. The amplitudes of calculated oscillations are in a close agreement with experimental data in



(a) 1.9 mm distant from the longitudinal axis (b) 0.7 mm distant from the longitudinal axis

Figure 7: Absolute longitudinal velocity variance of time averaged velocity

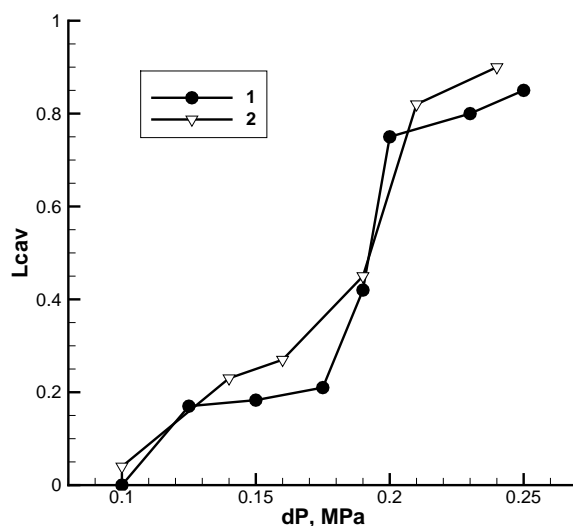


Figure 8: Dependence of dimensionless cavitation zone length on the pressure differential across the nozzle. 1 – experiment; 2 – simulation

the boundary layer of the flow, where the cavitation intensity is high. In the core area of the flow the calculated amplitudes are much weaker than those that are experimentally measured. This disagreement is due to attenuation of cavitation effects and the development of turbulent flow characteristics.

Acknowledgements

This study is supported by RFBR, research project No. 12-08-31264 mol_a.

References

- [1] I. Senocak, W. Shyy. Interfacial Dynamics-Based Modeling of Turbulent Cavitating Flows. Part-1: Time-Dependant Computations. *Int. J. for Num. Methods in Fluids*, 2004, 44, 975-995.

- [2] S. Gopalan, J. Katz. Flow structure and modeling issues in the closure region of attached cavitation. *Physics of Fluids*, 2000, 12(4), 895-911.
- [3] C.L. Merkle, J.Z. Feng, P.E.O. Buelow. Computational modeling of the dynamics of sheet cavitation. *Proceedings of third International Symposium on Cavitation*, Grenoble, 1998, 2, 307-311.
- [4] I. Senocak, W. Shyy. Interfacial dynamics-based modeling of turbulent cavitating flows. Part-2: Time-dependent computations. *Int. J. for Num. Methods in Fluids*, 2004, 44, 997-1016.
- [5] N.L. Markina, D.L. Reviznikov. Numerical simulation of fluid flow in the presence of cavitation. *Aerospace MAI journal*, 2011, 18(2), 200-210 (in Russian).
- [6] A. Sou, A. Tomiyama, S. Hosokawa, S. Nigorikawa, T. Maeda. Cavitation in a two-dimensional nozzle and liquid jet atomization (LDV Measurement of liquid velocity in a nozzle). *JSME International Journal*, 2006. 49(4), 1253-1259.
- [7] G.S. Nazarov, Experimental studies on cavitation characteristics of convergent nozzles. *Engineering-Physical Journal*, 1968, XIV(3), 423-429 (in Russian).

Nadezhda L. Zagordan, Institution of Russian Academy of Sciences Dorodnicyn Computing Centre of RAS, Vavilov st. 40, 119333 Moscow, Russia

Dmitry L. Reviznikov, Moscow Aviation Institute (National Research University), Volokolamskoe sh. 4, 125993, Moscow, Russia